Chemical Engineering Journal 497 (2024) 154962

Contents lists available at ScienceDirect

Chemical Engineering Journal

journal homepage: www.elsevier.com/locate/cej

Process stability in anaerobic Digestion: Unveiling microbial signatures of full-scale reactor performance

D. Santinello [a], G. Zampieri [a], S. Agostini [b,c], B. Müller [b], L. Favaro [c,d], L. Treu [a,*], S. Campanaro [a]

[a] Department of Biology, University of Padova, Via U. Bassi 58/b, 35121 Padova, Italy
[b] BTS Biogas s.r.l., Via Vento 9, 37010, Affi, VR, Italy
[c] Department of Agronomy Food Natural Resources Animals and Environment (DAFNAE), University of Padova, Agripolis, Viale dell'Università 16, 35020 Legnaro, PD, Italy
[d] Department of Microbiology, Stellenbosch University, Private Bag X1, Matieland 7602, South Africa

ARTICLE INFO

Keywords:
Anaerobic digestion
Biogas
Metagenomics
Process monitoring
Methanogenic archaea

ABSTRACT

Anaerobic digestion is responding to the growing demand for sustainability by exploring alternatives for methane production through renewable processes. The target is to implement stable production systems at industrial scale that can accommodate heterogeneous feedstocks with seasonal or intermittent availability. In this study, we investigated the microbiomes of six full-scale biogas plant digesters, operated under continuous production with distinct feedstock and varying operating parameters, by monitoring multiple time points over an 18-month period. This time-course experiment analyzed 114 Metagenome-Assembled Genomes alongside physico-chemical assessments to identify common and plant-specific indicators for operational management. Results identify a Limnochordia and a Dysgonomonadaceae bacteria, as well as *Candidatus* Methanoculleus thermohydrogenotrophicum, as widespread and potentially desirable components of the microbiota for resilient digestion of varying waste, including the peculiar olive pomace. The abundance of individual taxonomic groups and their reconstructed metabolic pathways aligned with the availability of their fermentation substrates, finding a prevalence of beta-oxidizing bacteria with lipid-rich olive pomace. Monitoring through perturbation events revealed possible causative and remediative microbiological factors, in particular *Methanosarcina flavescens* and *Candidatus* Syntrophosphaera thermopropionivorans could contribute to restoration of reactor performance. This work showcases relationships between digester operation and its microbiome, supporting microbial monitoring as a tool to increase biogas production efficiency.

1. Introduction

In recent years investments in the biogas production field have been gaining relevance in both the industry and scientific context [1]. Anaerobic digestion (AD) is a process mediated by microbial communities, which degrade organic matter to release biogas. AD plays a crucial role in promoting sustainable waste management practices, and generating renewable energy, thereby contributing to environmental protection and climate change mitigation [2]. Indeed, as agricultural, farm and organic waste can be converted to biogas in industrial AD scale, this process can provide an effective solution for managing waste streams, for example from the food supply chain [3]. Exploiting AD, organic matter is converted into biogas, resulting in a reduction of waste volume sent to landfills and minimizing uncontrolled methane (CH_4) emissions from decomposing organic matter [4].

Microbes partaking in AD perform one or more phases of the process: hydrolysis, acidogenesis, acetogenesis, and methanogenesis. Their role can be inferred by identifying metabolic pathways coded in their genome, allowing us to understand their contribution to the digestion process. As organic matter is degraded into simpler molecules, volatile

Abbreviations: SAOB, Syntrophic acetate oxidizing bacteria; SPOB, Syntrophic propionate oxidizing bacteria; SBOB, Syntrophic butyrate oxidizing bacteria; RA, Relative abundance; VFA, Volatile fatty acids; MAG, Metagenome-Assembled Genome; TAN, Total Ammonia Nitrogen; FAN, Free Ammonia Nitrogen; GTDB, Genome Taxonomy Database; KO, KEGG Orthology code; MIMAG, Minimum Information about a Metagenome-Assembled Genome.

* Corresponding author.
E-mail address: laura.treu@unipd.it (L. Treu).

https://doi.org/10.1016/j.cej.2024.154962
Received 18 April 2024; Received in revised form 1 July 2024; Accepted 18 August 2024
Available online 20 August 2024

fatty acids (VFA), carbon dioxide (CO_2), and hydrogen (H_2) are released by fermentative activity and CH_4 is generated by methanogenic archaea.

Interspecies relationships play a vital role in anaerobic ecosystems since they are key to the energy-extracting capacity of primary fermenters in microbial food webs and contribute to more efficient and complete oxidation of organic wastes [5]. Syntrophic oxidizing bacteria promote the activity of hydrogenotrophic methanogens by oxidizing VFA, and are known as Syntrophic Acetate (SAOB), Propionate (SPOB) or Butyrate (SBOB) Oxidizing Bacteria. It is therefore crucial for reliable and continuous biogas production that a balanced community be persistent in the reactor. Yet, the microbiome is not analyzed during regular biogas plant operation, possibly limiting plant performance as less desirable states of the community are not recognized. Indeed, microbiome monitoring could assist in identifying potential operational scenarios under conditions of inhibition by toxic biomass components or unbalanced parameters.

As for most industrial processes, well-defined practices like procedures, protocols, and quality standards throughout operations result in optimized resource utilization [6]. Standardization can identify and reduce inefficiencies, leading to improved biogas quality and maximizing resource recovery from organic waste streams in continuous production processes [7]. This can include inocula for reactor startup and augmentation, reducing the time needed for community adaptation thus optimizing performance by minimizing downtime [8].

Industrial AD of agricultural biomass is commonly performed in continuous stirred tank reactors (CSTR), guaranteeing optimal flow while avoiding problems that reactors such as upflow anaerobic sludge blanket encounter with solid contents [9]. Therefore, analyzing the microbiome of CSTR should prove to reveal trends in time of the microbiome, including stable and variable microorganisms. Indeed, variations in the feedstock of industrial digesters can result in alterations of the microbial community composition [10] and consequent process imbalances, like VFA accumulation [11], reducing the overall CH_4 production [12]. Monitoring the AD microbiome through time can help to decode boundaries within which the relative abundance (RA) of the core members of the community can vary and how specific players affect digesters operation and biogas production [10,13]. Due to its inherent flexibility, the microbial community can swiftly adjust its composition in response to fluctuations in feedstock and operating parameters. Nevertheless, severe disruptions to reactor operation can destabilize the existing equilibrium, requiring the microbiome a significant period to re-establish full operational capacity. Therefore, gaining a deeper understanding of how the microbiome evolves over time during reactor operation is crucial for enhancing process management.

Compared to amplicon-based analysis, reconstruction of Metagenome-Assembled Genomes (MAGs) allows the identification of individual microbes with great resolution and the estimation of their functional potential based on their gene content, gathering a deeper understanding of the "microbial black box" [14,15]. Thus, by relating MAG metabolic capabilities and abundance over time to reactor operation it is possible to hypothesize the microbial role in AD, paving the way for process optimization. Capturing the diversity and activity of microorganisms in full-scale digesters through metagenomics will allow the creation of databases for rapid and simple profiling of microbial communities. With well-defined reference databases and streamlined techniques, it is expected that microbial monitoring of AD plants will become an effective and feasible approach to sustain productivity through perturbations and fluctuations. Furthermore, defining a core set of bacteria and archaea consistently present in industrial AD environments regardless of feedstocks will be instrumental for determining the stability and resilience of AD systems. This knowledge will lead to increased yield in the biogas industry through unstable nutritional composition of the feedstock over time.

The aim of the current research is to link biological dynamics in industrial-scale AD with plant operation including feedstock compositions and performance. To this end, we analyzed the input, microbiome, products, and by-products of selected reactors comprising both widespread and less common feedstock over 18 months. By employing a genome-centric approach, we not only captured how microbial populations and their biological functions vary over time but also identified markers of seasonal fluctuations and major process perturbations, which could inform process management practices.

2. Materials and methods

2.1. Sampling and reactor operation

The selection of reactors included in the study considered feedstock characteristics, process efficiency, biogas yield, treatment capacity, and hydraulic retention time. After this screening, six reactors were selected from a panel of 12 preselected plants to maximize variability in feeding regimen, biochemical composition of the digestate, and performance. The digesters are hereafter identified by their operator: Agroenergy s.r.l. (AGR), Azienda Agricola La Carnita (SOR), Energie Rinnovabili Poggesi s.r.l. (ERP), Gallman Bioenergy (GAL), Produttori Energia Società Cooperativa Agricola (PRO), Società Agricola Green Energy s.r.l. (GRE). Structural and operative characteristics of the biogas plants have been noted (**Supplementary Materials**). Feedstock was calculated based on the mass of the different organic products introduced in the reactor in the week prior to the sampling point. Organic loading rate (OLR) was estimated through percentage of dry organic matter (oDM) of each feedstock component and total feedstock mass. Operational parameters and microbiome over time were monitored sampling from each reactor during 18 months from digestate. Sampling was performed at circa bimonthly intervals from august 2022 (T01) to february 2023 (T10) (**Supplementary Table S1**). Samples were frozen to −80 °C and stored until further analysis.

2.2. Chemical analyses

Feedstock characterization was performed as detailed in **Supplementary Materials** and, where needed, integrated with data from literature to obtain biochemical composition on dry matter (DM) basis.

VFA composition was determined using a PerkinElmer series 200 high performance liquid chromatography (HPLC) system equipped with a Biorad Aminex HPX-87H column (300 mm × 7.8 mm) and a UV/VIS detector 292N8091703E. The mobile phase was 0.015 M H_2SO_4 with a flow rate of 0.6 mL/min. The column oven was set at 60 °C. The following VFA were measured by this method: acetic, propionic, valeric, isovaleric, butyric and isobutyric. Additional details are reported in **Supplementary materials**. Samples of digestate were previously filtered, diluted and treated with potassium ferrocyanide and zinc sulfate solution to promote protein precipitation. Total Ammonia Nitrogen (TAN) was detected by photometric analysis with indophenol method, using the kit Nanocolor Ammonium 50 (MACHEREY-NAGEL GmbH & Co. KG, Germany). Free Ammonia Nitrogen (FAN) was then calculated with Eq.1 according to [16]:

$$FAN = TAN \times \left(1 + \frac{10^{-pH}}{10^{-\left(0.09018 + \frac{2729.92}{T}\right)}} \right) \quad (1)$$

where TAN and FAN are expressed as mg_N/L of digestate; T(K) represents recorded digestate temperature at sampling on the Kelvin scale and pH is measured pH of the digestate. Micronutrients were detected according to method DIN EN ISO 11885. Electric conductivity, redox potential, pH and FOS/TAC have been measured on digestates with the following instruments: WTW multi 350i – KM002/1 with TetraCon 325 electrode, Memocal T – KM025, pHmeter WTW multi 350i – KM002/2 with Sentix 41 pH electrode and titrator Titroline 6000 – KM105, respectively. Measurements of CH_4, O_2 and H_2S in the biogas was carried

out at the plant site using the system Awiflex (Awite, Germany). Further details can be found in the **Supplementary Material**.

2.3. Nucleic acid Extraction, sequencing and metagenomics

DNA extraction was performed in triplicates using the DNeasy PowerSoil Kit (QIAGEN, Hilden, Germany), following the recommended protocols. Illumina DNA libraries were prepared using the Illumina DNA Prep Kit and sequenced paired-end on an Illumina NovaSeq 6000 system (Illumina Inc., San Diego, CA). Illumina sequencing yielded an average of 12 million reads per sample. Nanopore sequencing was performed on the first sample from each reactor. Nanopore libraries were prepared with kit SQK-LSK109 and sequenced with a FLO-MIN106 R9 flow cell on a MinION device (Oxford Nanopore Technologies, Oxford, UK), with 30 % of the reads above Q10. A genome-centric approach was followed as previously described [17]. Briefly, Illumina reads from timepoints T01 to T04 of all reactors were co-assembled; Nanopore reads were co-assembled and polished. The short and long read assemblies were merged. Contigs were separated into bins to create Metagenome-Assembled Genomes (MAGs) using multiple binning tools in parallel and dereplicated (see **Supplementary Material** for details). Only MAGs with medium and high-quality according to Minimum Information about a Metagenome-Assembled Genome (MIMAG) specification [18] were further processed. RA of the MAGs was determined with CheckM *coverage*. Shannon's Alpha diversity was calculated with *phyloseq* [19], using a synthetic read count normalized by MAG length.

MAGs taxonomy was assigned against GTDB (Genome Taxonomy Database) taxonomy v214 [20] with GTDB-Tk v2.3.2 while comparison of MAGs with the AD database [21] was performed with dRrep 3.2.2 [22] at species level (Average Nucleotide Identity, ANI, 0.95). Functional potential was assessed on the matched MAGs from the database if their quality was higher according to CheckM2 [23]. This allowed functional annotation to be performed on a set of 114 MAGs of which 96 were predicted by CheckM2 to be over 90 % complete while only 7 had more than 5 % contamination, ensuring reliable functional potential estimation. Prodigal v2.6.3 [24] and eggnog-mapper v2.1.7 [25] were used to predict the open reading frames and annotate them, while carbohydrate active enzymes (CAZymes) were extracted locally with an Hidden Markov Model (HMM) search against the dbCAN HMM database release 12.0 [26]. The Kyoto Encyclopedia of Genes and Genomes (KEGG) [27] was used as a reference database for pathways and modules. Custom modules for butyrate oxidation ("ButOx") and the alternative syntrophic acetate oxidation pathway (Wood–Ljungdahl/glycine cleavage system, "WL/GCS") were implemented using KEGG Orthology codes (KOs) identified in KEGG map00650 and map1200, respectively (**Supplementary Table S2**). For prediction of KEGG module completeness, block completeness was manually calculated according to KOs. Modules were considered present if all blocks were present or a maximum of one block was missing (1-bm). Phylogenesis was assessed using PhyloPhlAn 3.0.51 [28] and the tree was visualized using iTOL v6.5.8 [29]. Extracellular proteins were predicted with PSORTb 3.0 [30] using the gram staining parameter as predicted by Traitar [31], and peptidases/proteases were identified by manual refinement of eggnog annotation.

2.4. Statistics, metabolic Reconstruction, and visualization

Ordinations and multivariate analyses were performed using the *vegan* 2.6–4 R package [32]. Microbiome beta diversity was performed using the Bray-Curtis dissimilarity and visualized with a Non-metric Multidimensional Scaling (NMDS). PERMANOVA and beta-dispersion analyses were performed with 9999 permutations. Prior to Principal Component Analysis (PCA) and environmental variable fitting, compositional values were normalized through the robust Centered Log Ratio transformation, while values of operational parameters were standardized. Upset plot visualization was created with package UpSetR [33]. Functional enrichment of a set of MAGs was performed with EnrichM 0.6.0–3 [34] through Fisher's exact test. The set of enriched genes was then manually analyzed through KEGG Mapper. For description of microbiome functions, the percentage of community bearing a given module was calculated by summing the RA of all MAGs of the "dominant" subset (1 1 4) that were estimated to possess the module. Correlations were computed as Spearman's ρ.

3. Results and discussion

3.1. Reactors characteristics and operation

Six digesters from agro-industrial AD plants were monitored analyzing the digestate physico-chemical parameters and the microbiome composition, as well as reactor temperature and biogas composition (Table 1). The monitoring period spanned 18 months with ten bimonthly sampling points for AGR, GAL, PRO, GRE, nine for ERP and eight for SOR (indicated as T01 to T10). All digesters were CSTRs operated between 42° and 48 °C, a temperature range between mesophilic and thermophilic reported to be highly effective for the AD process [35]. During the monitored period, the reactors operated with vastly different biomasses with a largely stable energy production (**Supplementary Figure S1**). Indeed, in this study the biogas plants were selected to maximize diversity in the feedstock in order to cover a wide array of agro-industrial AD systems, some of them having a seasonality in the inputs. Feedstocks directly influence process efficiency, biogas yield, and overall system performance, as its organic composition and degradation rate affect microbial dynamics and biogas production potential [36]. Therefore, such difference in the feedstock can help to understand which microorganisms represent a dominant core microbiome of AD regardless of the organic matter being digested and, conversely, which species are most suited for operation of digesters with specific inputs. Briefly, GAL exclusively utilized silage, ERP supplemented silage with hay, SOR utilized a substantial portion of cow manure co-digested with silage. These represent a common feedstock of agro-industrial AD plants. GRE co-digested chicken manure and silage in roughly equal proportions, while PRO supplemented silage with chicken manure and seasonal vegetables. Chicken manure is a peculiar feedstock due to its high content of proteins and uric acid, which results in elevated nitrogen levels possibly leading to process inhibition [37]. Lastly, AGR exclusively digested two-phase olive pomace, an organic-rich and valuable biomass seldom utilized in AD processes due to the scarce nitrogen content, high levels of toxic phenolic compounds and potential lipid overload [38]. PCA highlighted that the biochemical composition of AGR feedstock notably differed from other plants, with a higher presence of lipids (approx. 14 % oDM) as a consequence of the olive pomace (Fig. 1**A**). Digesters with a main contribution of silage (ERP, GAL, PRO) were rich in starch (approx. 30 % oDM), a source of fermentable carbohydrates present in various organic substrates. Reactors GRE and SOR presented a higher component of proteins (approx. 20 % oDM) owing to the substantial feeding of animal manure. Detailed feedstock composition is reported in **Supplementary Table S3.**

During the monitoring period all reactors operated stably except for two main events. First, the ERP plant was affected by engine failure at T06. This time point was characterized by a decrease of temperature (−5.3 °C), CH_4 yield (−3.3 **%**) and organic loading. Reactor SOR experienced an acidification event at T07, which nonetheless did not reduce the percentage of CH_4 in the biogas. These events represented points of interest for evaluating microbial stability through AD failure and recovery periods. Among the reactors, feedstock variability differed, as AGR and GAL were stably fed with a single biomass, ERP varied considerably in correspondence with operational issue, both in composition and OLR, where only hay was used as biomass (**Supplementary Figure S2**). A PCA was performed on digesters according to selected operational parameters (Fig. 1**B**). Three groups of vectors could be identified: I comprising temperature and CH_4 percentage, II including

Table 1
Summary of major feedstocks and main operational parameters of the monitored digesters in the six full-scale biogas plants. Parameters are reported as average over the period ± standard deviation.

	AGR	SOR	ERP	GAL	PRO	GRE
Feedstock	Two-phase olive pomace	Cow manure, silage	Silage, hay	Silage	Silage, vegetables, chicken manure	Chicken manure, silage
VFA (mg/L)	71 ± 24	3062 ± 2448	259 ± 174	98 ± 109	679 ± 804	2708 ± 845
FOS/TAC	0.33 ± 0.02	0.51 ± 0.17	0.25 ± 0.05	0.24 ± 0.3	0.24 ± 0.03	0.31 ± 0.05
Solids (%)	8.1 ± 0.1	9.0 ± 0.4	8.0 ± 0.7	9.5 ± 0.9	10.2 ± 1.3	8.3 ± 0.6
TAN (mg_N/L)	387 ± 65	1720 ± 140	1828 ± 295	2168 ± 273	3867 ± 261	4432 ± 366
FAN (mg_N/L)	48 ± 15	147 ± 89	198 ± 55	295 ± 107	702 ± 127	960 ± 149
CH_4 (% in biogas)	60.4 ± 1.1	51.1 ± 1.7	50.0 ± 1.5	51.6 ± 1.4	50.4 ± 1.3	50.6 ± 1.2
T (°C)	45.8 ± 0.4	45.0 ± 0.0	45.1 ± 1.9	48.0 ± 1.1	43.5 ± 1.0	42.7 ± 0.4
pH	7.8 ± 0.1	7.6 ± 0.3	7.7 ± 0.1	7.8 ± 0.1	8.1 ± 0.1	8.2 ± 0.1

pH, Total Ammonia Nitrogen (TAN), Free Ammonia Nitrogen (FAN), and percentage of H_2S, III consisting of VFA and their indicators (FOS and FOS/TAC). These serve as indicators for possible inhibition [39] and are related to digester stability, aiding in predicting process upsets [40]. Substantial differences determined the separation of the biogas plants along PC1, which was contributed by most of the tested parameters except for VFA and FOS/TAC, which contributed to PC2. The large contribution of TAN and FAN to reactor separation is expected owing to the vast differences in nitrogen compounds between the two distinctive feedstocks: olive pomace and chicken manure. While nitrogen is required for the AD process for incorporation in biomolecules like amino acids and nucleotides, free ammonia represents the main inhibitor to the process due to its non-ionic diffusion and accumulation in the cell [41]. Elevated FAN especially affects aceticlastic methanogens at thermophilic temperatures and promotes hydrogenotrophic methanogenesis mediated by SAOB [42,43]. AGR and GRE were the most dissimilar reactors. In particular, AGR had the lowest VFA (~70 mg/l) and FAN (~48 mg/l) content, while FAN levels were highest in GRE and PRO reaching concentrations commonly regarded as inhibitory (1139 and 818 mg/l respectively) [41]. GRE and SOR had the highest VFA content (1759 and 2134 mg/l respectively). Data confirmed that the digesters had vastly different operational parameters, determining a very extended range of environmental conditions to be analyzed. Plants also varied in the parameter stability, AGR displayed highest stability, while GRE and PRO experienced the greatest fluctuations as evidenced by beta-dispersion **(Supplementary Materials, Supplementary Table S4, Supplementary Figure S3)**. SOR showed slow but marked shifts in VFA levels, with an acidification event in T07 where the content peaked at 9372 mg/l. Detailed measurements of operational parameters are reported in **Supplementary Table S5**.

3.2. Microbiomes diversity and correlations

Genome-centric metagenomics with hybrid Illumina-Nanopore sequencing approach allowed reconstruction of 529 dereplicated mid-to-high-quality MAGs, 149 (~28 %) of which were novel compared to the Biogas Microbiome Database comprising 314 CE reactors [21]. Alpha diversity calculated on these MAGs revealed AGR and SOR to have richer communities (**Supplementary Figure S4**). Overall, alpha diversity appeared to be higher in reactors with lower FAN levels, possibly due to the selectivity imposed by high ammonia concentration. PRO displayed the lowest diversity as MAG Limnochordia sp. BTS_001 dominated the community, reaching 31 % RA. A reduced set of 114 MAGs (referred to as "dominant MAGs") was obtained by selecting those having RA over 1 % in at least one sample, together with all archaea identified. These MAGs were largely of high quality (**Supplementary Table S6**) according to MIMAG standards [18] and accounted on average for 59.7 ± 3.27 % of the microbiome in each reactor (**Supplementary Materials**). This selection of relevant microbes was used for all downstream analysis: 107 (94 %) could be assigned at genus level against GTDB and 88 (77 %) at species level. These results highlight the power of genome-centric metagenomics for the reconstruction of microbiomes, allowing accurate identification both for novel and previously described species. In fact, 19 dominant MAGs represented novel taxa with respect to the Biogas Microbiome Database and their cumulative RA was higher in AGR (18.47 %) and GRE (10.45 %). This novelty is likely explained by the feedstock: AGR digested two-phase olive pomace, an uncommon biomass for agro-industrial AD plants, while the elevated loading of chicken manure in GRE determined extreme FAN levels. Based on these findings, it is evident that the microbiome of AD has not yet been thoroughly explored and further studies should expand the knowledge base by investigating the communities involved in digestion of less common organic waste.

A beta diversity analysis highlighted different communities existing in the six reactors (PERMANOVA $R^2 = 0.8$, $p = 0.001$). AGR and GRE possessed the most unique and divergent communities, while SOR, ERP and GAL communities were more similar yet still maintained distinctive compositions (PERMANOVA $R^2 = 0.44$, $p = 0.001$ – Fig. 1**C**). Interestingly, the relative positioning digesters by microbiome composition reflected the positioning by operational parameters, highlighting the interconnection between the two. Indeed, temperature and ammonia were previously identified as main factors in determining the composition of the AD microbiome [21,44]. However, microbiome clustering also reflected major feedstock composition: the microbial communities involved in digesting silage (GAL, ERP) and those co-digesting cow manure and silage (SOR) were more similar when compared against reactors co-digesting chicken manure (PRO, GRE) and olive pomace (AGR), which exhibited markedly different microbiomes. These findings suggest potential strategies for selecting inoculants to minimize the time required for community adaptation. Specifically, less common feedstocks such as olive pomace and chicken manure, which present greater challenges, may benefit from tailored inocula. Beta diversity of the 10 methanogenic archaeal MAGs largely confirmed the inter-cluster relationships found for the full set of dominant MAGs, though with less marked differences between reactors (Fig. 1**D**). Considering results from a beta-dispersion analysis, the microbiome of AGR and ERP was found to be less stable as compared to the others **(Supplementary Materials, Supplementary Figure S3, Supplementary Table S7)**. Reactor AGR displayed a seasonality trend, as community at points T01 to T03 resembled T07 to T08, while T04 to T06 located closest to T10, coherently with a yearly fluctuation **(Supplementary Figure S5)**. This could be linked with pomace storage, as will be discussed in paragraph 3.6.1. ERP microbiome variability could be attributed to points T06 and T07, corresponding to the engine failure and following time point. The community appeared altered by the lowering of the temperature and the change in feeding regimen at T06, yet reverted within a 4-month timeframe after a temporary state at T07. The microbiome of PRO displayed the third highest variance, although permutation analysis didn't prove it to be different from the more variable (AGR, ERP) or less variable microbiomes. PRO co-digested vegetables according to seasonal availability, suggesting a role of feedstock in affecting microbial stability. Conversely, parameter stability did not appear to affect the microbial dynamics. Aside from these variable microbiomes, an interesting trend was observed for SOR. While displaying the most stable

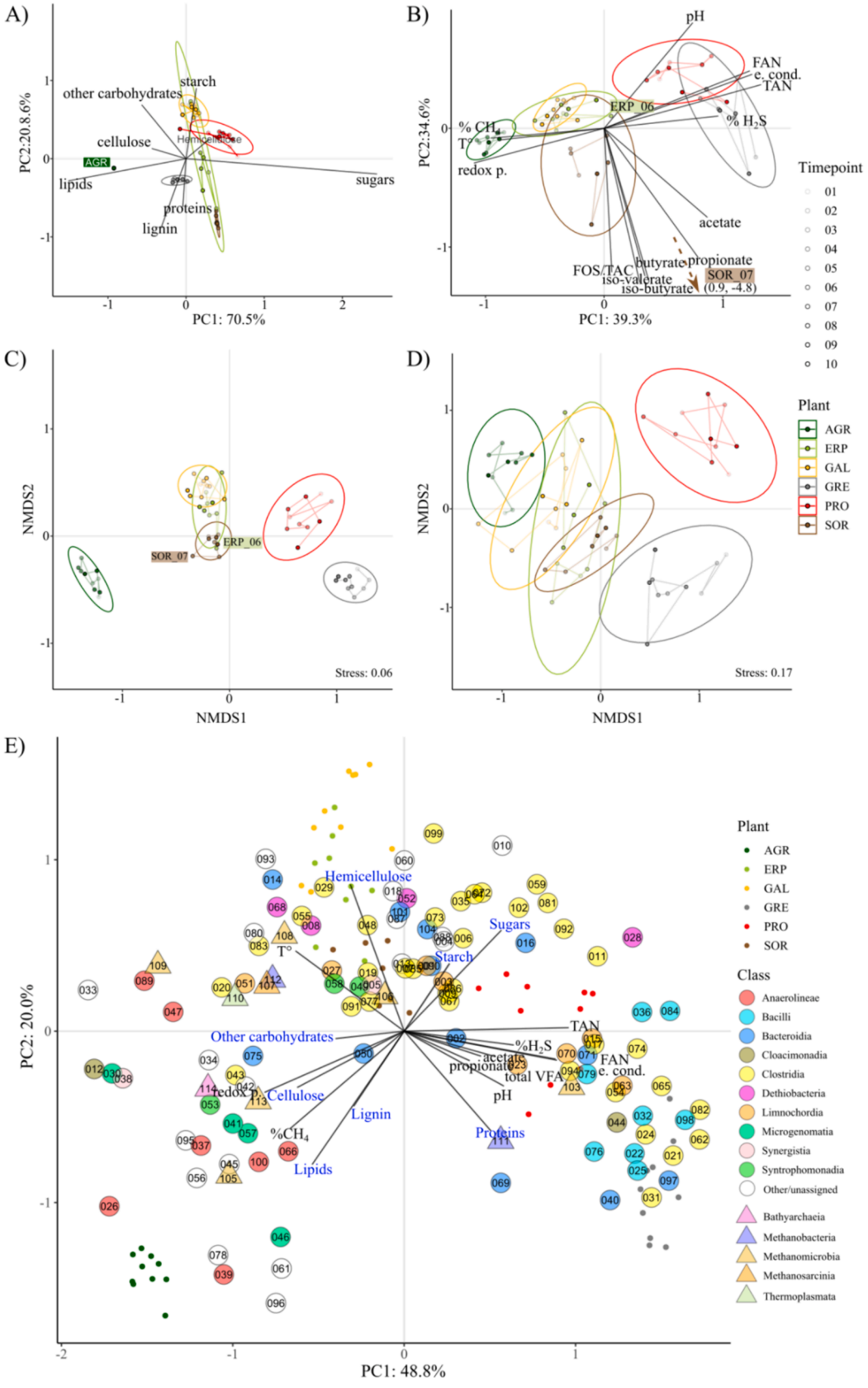

(caption on next page)

Fig. 1. Reactors variability according to feedstocks, operating parameters and community. (A) Biplot representation of digester clustered by feedstock biochemical composition. All points of the AGR plant are overlapping, as the feedstock was constant and monitored once. In plots A-D the color saturation of the dots increases from the first to the last sampling point. (B) Biplot representation of digesters clustered by selected operating parameters. Point T07 of SOR, corresponding to acidification, was an extreme outlier and it is not reported for overall clarity. (C) Beta diversity of the dominant MAGs and (D) Beta diversity of the 10 methanogenic archaea identified. In plots A to D, confidence ellipses for each plant are drawn at a 0.95 confidence interval of a multivariate t-distribution. (E) Relationship between community variability and measured parameters. Only parameters with a significant correlation to the ordination axes (p-value < 0.05) have been reported. The text is colored in blue for feedstock components vectors and in black for operational parameters vectors. The position of reactor PCA points has been scaled by 0.5 for visualization clarity. "e. cond": electric conductivity, "redox p".: redox potential.

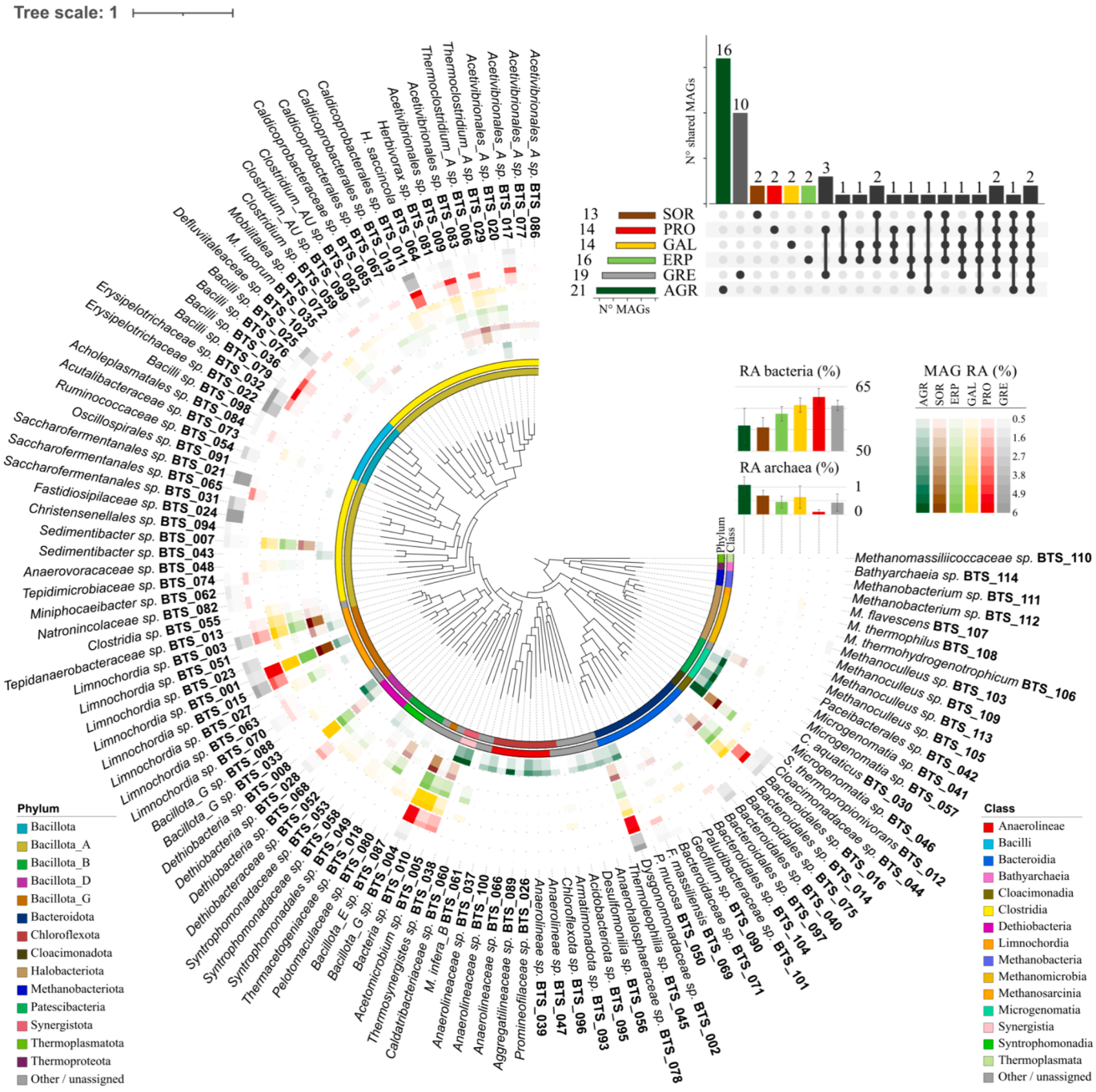

Fig. 2. Phylogenetic tree of the dominant MAGs. For each MAG, phylum and class are represented in the inner circles, while average and maximum RA in each reactor is represented by the intensity of the reactor's color in the external circles. Cumulative bacterial and archaeal MAG RA per reactor is represented by a bar chart. Note: MAG Paceibacterales sp. BTS_034 was not included in the tree. Shared and exclusive dominant MAGs, based on a threshold of average RA in the reactor greater than 1%, are represented with an UpSet plot.

community over the monitored period, a divergence was observed at T07 (acidification event), preceded by an apparent minor shift at T06 possibly contributing to the unbalanced state.

Furthermore, the communities were investigated in relation to feedstock biochemical composition and digester operational parameters to unveil potential connections between taxa and conditions within the system (Fig. 1**E**). TAN was found to explain the largest variability in the microbiome, while lipids were the most impactful digestion substrate. While VFA were found to significantly relate with microbes, the FOS/TAC indicator commonly used for process monitoring showed no significant relationship. Some taxa were found to have a defined pattern of abundance: MAGs of class Bacilli appeared to be positively associated with VFA concentrations, nitrogen levels and protein percentage in the feedstock. Classes Anaerolineae and Microgenomatia MAGs formed a well separate cluster positively associated with lipids in the feedstock and negatively associated with FAN and acetate. Conversely, MAGs of class Limnochordia and Clostridia were largely distributed with no specific environmental association.

3.3. Core community members

The analyzed microbial communities presented a high compositional heterogeneity (Fig. 2). Only 2 MAGs were found to be above 1 % average RA in all reactors and in almost all samples (52 and 47 out of 57): Limnochordia sp. BTS_001 and Dysgonomonadaceae sp. BTS_002, which were the overall most abundant with average RA 6.70 and 2.54 %, respectively (Fig. 3**A**). When compared against the Biogas Microbiome Database encompassing over 300 full-scale and lab AD reactors [21], Limnochordia sp. BTS_001 matched (ANI>99 %) the most widespread microorganism identified, that was previously classified as DTU010 sp002391385. Similarly, for Dysgonomonadaceae sp. BTS_002 and the top most abundant MAGs, trends of dominance suggest that these MAGs can be considered as part of the core microbiome, i.e. taxa that are present in a continuous AD system regardless of the feedstock used. Given their high abundance, they represent a crucial contribution to achieve stable and continuous production in AD plants. There is no precise information about the role of Limnochordia in AD, but this class has been commonly found in biogas-producing communities [17,45–47]. Several studies at laboratory scale suggested DTU010 sp002391385 to thrive in homoacetogenic or SAOB roles, as well as partaking to the higher stages of the AD funnel by metabolism of carbohydrates [48–50]. This hypothesized metabolic flexibility could be the explanation for the wide dominance of this taxa. Dysgonomonadaceae is a syntrophic family present in anaerobic environments, including AD systems. These species are responsible for the breakdown of complex organic compounds in the initial stages of the AD process and their fermentation to VFA [51,52]. Indeed, the highest average RA of Dysgonomonadaceae sp. BTS_002 was recorded in PRO (5.43 %), which exhibited the second highest non-fibrous carbohydrate content, and its abundance dropped at T10 along with carbohydrate content in the feedstock. Indeed, the abundance of the MAG was found to positively correlate with the percentage of sugar in the feedstock (ρ_s 0.73, p-value 0.016). Significant positive correlations were also found with hemicellulose and other carbohydrates in reactor SOR, where correlation with sugars was negative (**Supplementary Figure S6**).

3.4. Distinctive microbial members

The distinctiveness of communities within AGR and GRE was further confirmed by the uniqueness of MAGs with average RA over 1 %. In both reactors, most MAGs satisfying this threshold were not shared with other reactors (Fig. 2). This diversity is likely explained as the two reactors represent the two extremes in FAN content in the examined panel (Fig. 1**B**), which explained most of microbiome variability and is a known powerful driver of selection for microbial diversity [44]. This happens in addition to the intrinsic dissimilarities between the microbiomes of olive pomace and chicken manure compared to silage.

Indeed, AGR appeared to possess the most unique microbiome, with the dominant MAG being *S. thermopropionivorans* BTS_012 (average RA 5.85 %). This MAG was classified as *Candidatus* Syntrophosphaera thermopropionivorans, a putative SPOB isolated from thermophilic biowaste-digesting AD reactor [53]. Other dominant MAGs in AGR were largely absent or non-dominant in other reactors, including *Thermosynergistes* sp. BTS_038 (order Synergistales), which was the second most abundant MAG in the reactor (average RA 3.41 %), and several Anaerolineae (phylum Chloroflexota) and Microgenomatia (phylum Patescibacteria) MAGs. The presence of these MAGs in AGR draws similarities between the microbiome from this reactor, the microbiome of wastewater treatment plants (WWTP), and AD plants digesting activated sludge. This finding could be explained by the high lipid content of the substrates, indeed both Synergistales and Anaerolineales MAGs were highly present in communities treating synthetic lipid-rich wastewater [54]. Anaerolineae strains isolated from WWTP are reported as strict anaerobes with fermentative growth on carbohydrates and/or peptides, and putative syntrophic with hydrogenotrophic methanogens [55]. They were also enriched in alkane-degrading communities [56] and highly abundant in full-scale AD reactors treating activated sludge, where they were hypothesized to represent primary fermenters [57,58]. Patescibacteria are found in WWTP activated sludge, where they are hypothesized to act as symbionts or parasites owing to the limited pathways encoded by their small genome [59–61]. These observations explain the dissimilarities between reactor AGR and the other reactors, as WWTP-based AD systems were found to possess a highly different core microbiome than farm-based ones [62].

Conversely, reactors GRE and PRO shared a substantial fraction of the community with ERP, SOR and GAL in species of class Clostridia, while they were characterized by the class Bacilli including Erysipelotrichales and Saccharofermentanales (Fig. 2), with Fastidiosipilaceae sp. BTS_024 as the most abundant MAG (avg RA 7.60 %). Erysipelotrichaceae are associated with animals, including chicken gut [63]. As chicken manure represents a substantial percentage of the biomass digested by GRE and PRO reactors it is plausible that Erysipelotrichaceae colonization may be due to the inflow of chicken manure.

3.5. Microbial abundance dynamics in time

MAGs displayed different trends of stability over time (Fig. 3**B**). Specifically, Limnochordia sp. BTS_001 appeared to follow a seasonality trend, as its abundance was highest from August to December in all reactors (**Supplementary Figure S7**). Particularly, in PRO it fluctuated from 5.77 % to 31 %, therefore potentially affecting the process. Its abundance was found to correlate with TAN levels and temperature (**Supplementary Figure S8**) while no correlation with feedstock was identified**.** On the contrary, Dysgonomonadaceae sp. BTS_002 was stable in abundance, with only a few transient increases (see 3.6.2).

Distinctly from the other reactors, MAGs in AGR presented an unstable abundance over time, often reaching high RA in few points. These fluctuating abundances, together with the seasonality variations, explain the high richness of species observed. This effect can be attributed to the annual storage of olive pomace, while the point variability of MAGs is more puzzling considering the stability of the reactor. The peculiar Microgenomatia MAGs ranked among the most variable MAGs both in the reactor and also in the entire study, while Anaerolineaceae MAGs varied in stability, but cumulatively displayed a strong seasonality (**Supplementary Figure S5**). Among the predominant MAGs, Promineofilaceae sp. BTS_026, *S. thermopropionivorans* BTS_012 and Dysgonomonadaceae sp. BTS_002 were the most stable, suggesting an enduring contribution to the reactor activity.

In GRE, the two most abundant MAGs displayed opposite behaviors: Fastidiosipilaceae sp. BTS_024 displayed wide variations (2.9–14.3 % RA), with a higher abundance from February to June, while Saccharofermentanales sp. BTS_021 was the most stable of MAGs with average

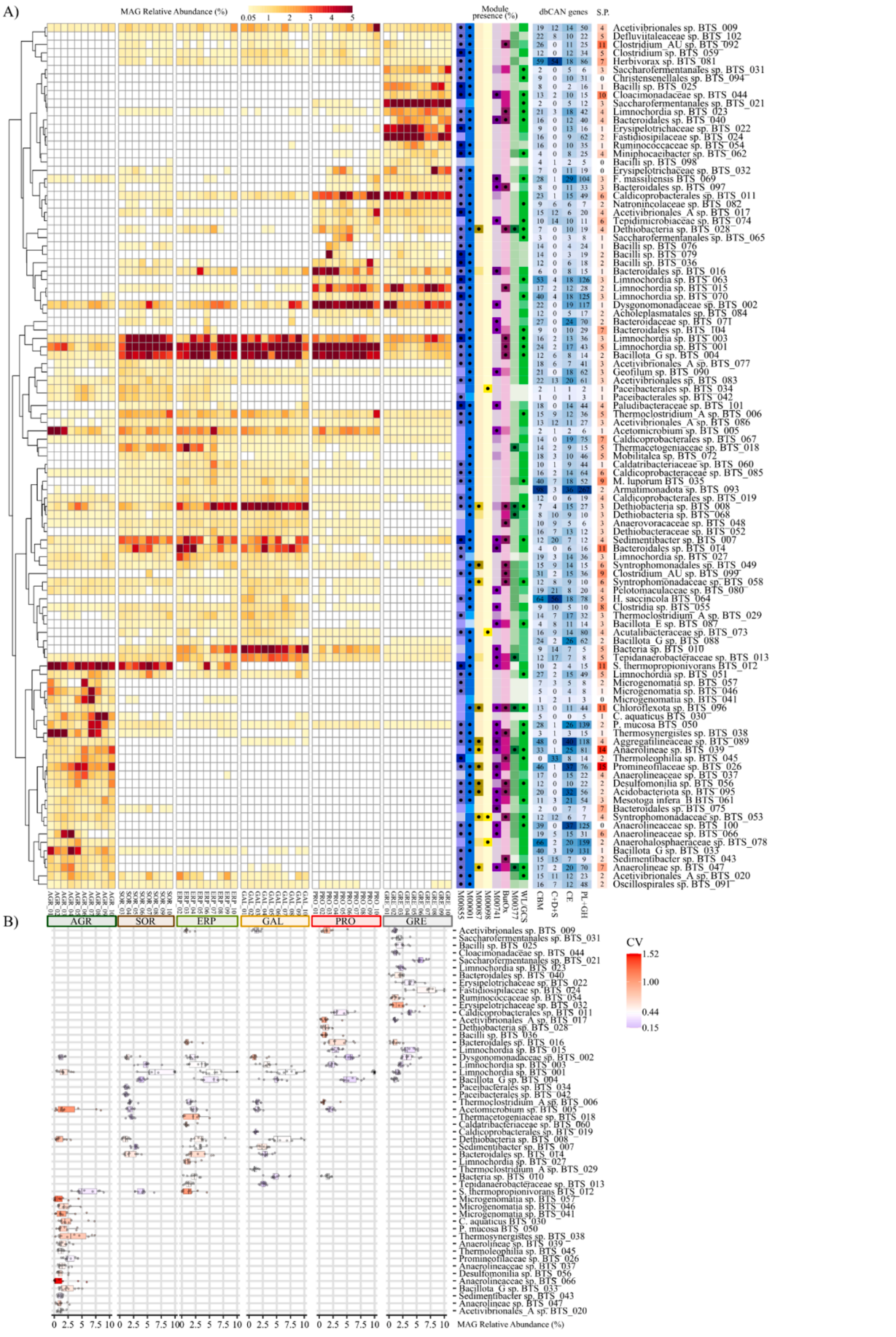

(caption on next page)

Fig. 3. Abundance and functional potential of the dominant bacterial MAGs. MAGs were clustered using Pearson correlation with complete clustering. A) From left to right: a heatmap visualizing RA in each sample; completeness of selected KEGG and custom modules, on 4-step color scales, with a dot indicating complete or 1-bm module (M00855: Glycogen degradation, M00001: Glycolysis, M0087: beta-Oxidation, M00098: Acylglycerol degradation, M00741: Propanoyl-CoA metabolism, ButOx: custom defined butyrate oxidation module, M00377: Reductive acetyl-CoA pathway, WL/GCS: custom defined WL/GCS module); number of genes positive for dbCAN hits (CBM: carbohydrate-binding module, S+C+D: summed S-layer homology domain, cohesin and dockerin, CE: carbohydrate esterases, PL+GH: summed polysaccharide lyases and glycoside hydrolases); number of genes predicted to encode for secreted peptidases (S.P.). B) Stability over time of MAGs with average RA greater than 1 %. The profile of each MAG's RA within a reactor is represented as a boxplot. Values exceeding the x-axis limit (10 % RA) are squashed and represented with an "x" symbol. The coefficient of variation (CV) of each MAG is represented on a color scale centered on the median CV of the MAGs plotted.

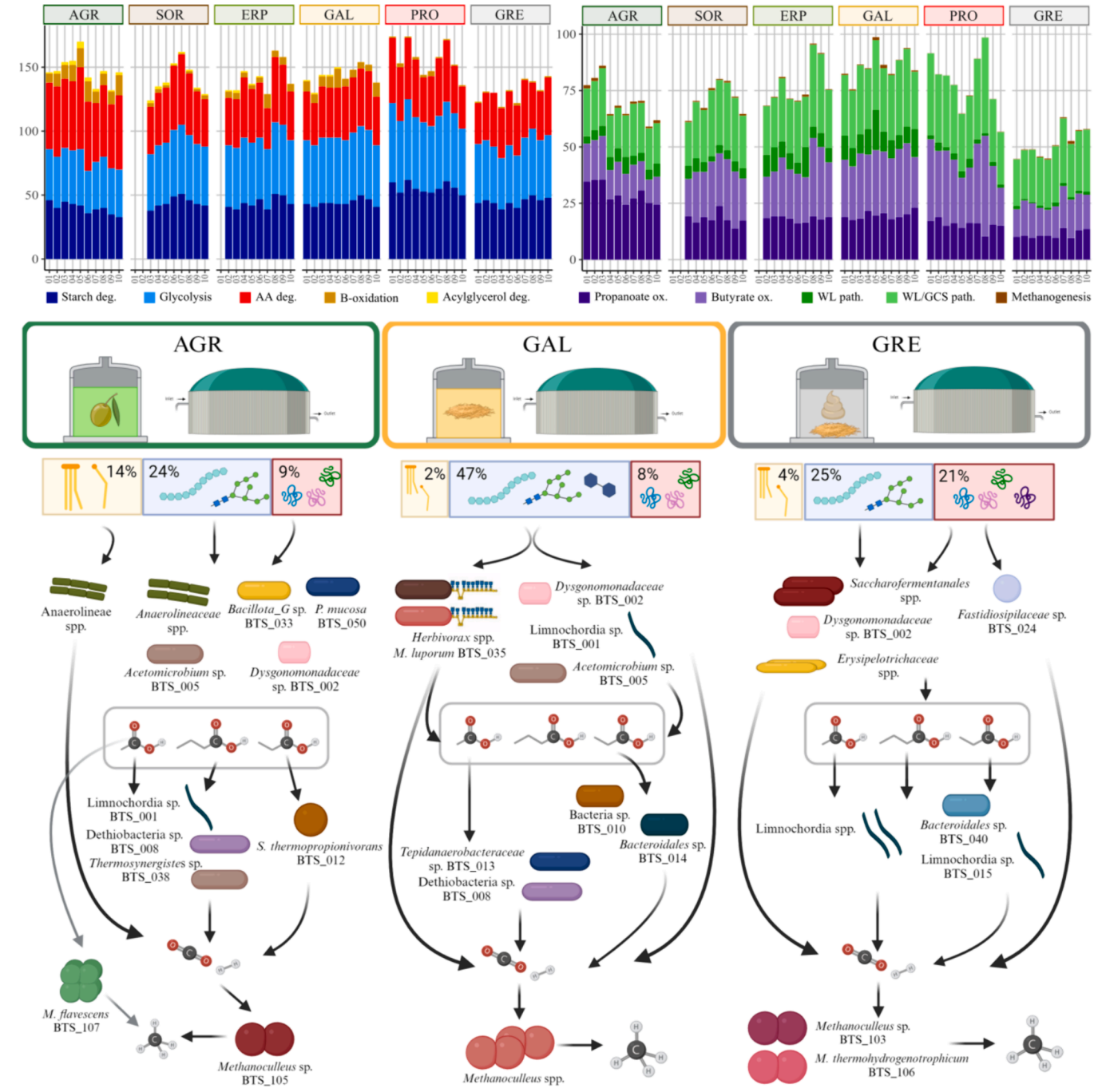

Fig. 4. Functional composition of the different communities. Data reported in the top part of the figure visualizes cumulative RA of MAGs harboring modules involved in substrate degradation and intermediate metabolism (complete or 1-block missing) as follows: Starch deg: M00855; Glycolysis: M00001; AA deg.: sum of M00035, M00036, M00044, M00045, M00956, M00957, M00960, M00970); B-oxidation: M00087; Acylglycerol deg.: M00098; propionate ox.: M00741; butyrate ox.: custom module ButOx, WL: M00377, WL/GCS: custom module WL/GCS; methanogenesis: cumulative RA of the identified methanogens). Lower part of the figure is a schematic representation of the functional profile of the dominant species in reactors AGR, GAL and GRE, reporting from top to bottom the more relevant MAGs involved in hydrolysis, VFA production/transformation and methanogenesis. Reconstruction is based on functional annotation and literature.

RA>1%. The MAGs of SOR displayed a rather stable abundance, indicating no nexus with the fluctuating parameters, with the exception of the acidification event at T07 that will be discussed in more detail in section 3.6.2.

3.6. Microbiome functional composition and enrichment

To link microbial functional potential with reactor performance, functional annotation was performed on the dominant MAGs (Fig. 3**A**). Annotation of the two ubiquitous MAGs was coherent with the literature findings. Limnochordia sp. BTS_001 possesses an almost complete custom module for butyrate oxidation, highlighting a potential activity as SBOB. While the WL pathway for acetate oxidation was incomplete, SAOB activity could be performed through the proposed alternative WL/GCS pathway, which was found. Both butyrate and acetate utilization were previously predicted through flux balance analysis [50]. Further, a moderate number (43) of glycoside hydrolase (GH) genes were identified, compatible with a role in the first stages of AD. The hydrolytic role of Dysgonomonadaceae sp. BTS_002 was supported by an elevated number of predicted CAZymes. The M00741 module (propanoyl-CoA metabolism) was almost complete, and crucially the two blocks identified are also involved in propionate production likely from its activity as fermentative bacteria. Notably, abundance of this MAG in SOR spiked (3.67 %) at T07 corresponding to reactor acidification, possibly contributing to the excess of VFA, as its abundance was positively correlated with propionate levels (ρ_s 0.71p-value 0.046, **Supplementary Figure S8**). To clarify the interconnection between feedstock, operational parameters and microbiome, the functional makeup of the peculiar microbiomes was examined more in detail (Fig. 4).

3.6.1. Olive pomace digesting community

AGR was characterized by the highest abundance of MAGs with predicted beta-oxidation, acylglycerol degradation and propionate oxidation pathways. As reported before, the feedstock of AGR is two-phase olive pomace, a lipid-rich waste where acylglycerols can therefore represent an important energy source for the microbial community [64]. Efficient degradation of acylglycerols is essential for maintaining process stability and maximizing biogas yield in AD systems [65]. The beta-oxidation pathway was also identified in four Anaerolineae MAGs, linking their presence in reactor AGR with the lipid-rich feedstock. Of these, Promineofilaceae sp. BTS_026 and Aggregatilineaceae sp. BTS_089 also encoded the propionate oxidation module. The three MAGs lacking beta-oxidation (Anaerolineaceae sp. BTS_037, Anaerolineaceae sp. BTS_066, Anaerolineaceae sp. BTS_100) formed a separate cluster on the phylogenetic tree (Fig. 2), possibly representing a group of species with a different metabolism within Anaerolineae. We can therefore hypothesize Anaerolineae bacteria to perform various roles in the upper stages of AD, including lipid oxidation and carbohydrate fermentation. Other MAGs with predicted beta-oxidation included three Syntrophomonadales, two of them assigned to family Syntrophomonadaceae, which was demonstrated to perform fatty-acid oxidation and syntrophic growth on butyrate [66]. Syntrophomonadaceae sp. BTS_053 also encoded the acylglycerol degradation module as 1-bm. The seasonality trend observed from the beta diversity analysis is reflected in the functional potential. Abundance of the propionate oxidation module appeared to increase in the period spanning August to December (T01-T03, T07-T09), with *S. thermopropionivorans* BTS_012 and Thermosynergistes sp. BTS_038 contributed in both years. A similar trend was observed for the WL/GCS module. Conversely, abundance of bacteria encoding the beta-oxidation pathway was higher from February to June (T04-T06, T10) with the main contribution of Promineofilaceae sp. BTS_026. These dynamics could be determined by chemical modification of the feedstock associated with the storage of olive pomace over the year [67], as fresh pomace is obtained in the final months of the year and the reactor is gradually switched from the old to the fresh pomace.

3.6.2. Silage and manure digesting community

SOR had a functional profile akin to the chicken manure digesting reactors GRE and PRO, suggesting the predominant contribution of animal manure. Increased RA of both hydrolytic-fermentative and VFA oxidizing microbes was observed from T06 to T08, encompassing the acidification event at T07. This mirrored a decrease in alpha diversity and community heterogeneity (**Supplementary Figure S4**), being therefore notably linked to reactor acidification. The reduction in microbiome complexity appears as a putative factor affecting the stability of the continuous AD process and underlines microbial monitoring as a relevant tool for early warning.

Moreover, propionate oxidation increased in RA steeply at T07 without a preceding trend, suggesting a response to the elevated VFA levels. This was mainly attributed to *S. thermopropionivorans* BTS_012 at its maximal abundance (RA 6.23 %) as the most abundant MAG, showcasing an interesting role in remediating the propionate accumulation. Conversely, Dysgonomonadaceae sp. BTS_002 presented a sharp peak, likely contributing to acidification through its fermentative activity (**Supplementary Figure S9**). Given its involvement in acidification, this organism could represent a factor to monitor for imminent acidification.

In reactor ERP, the functional makeup of the community was affected by the temperature drop and alteration to the feeding regimen at T06. A sudden spike in RA of *S. thermopropionivorans* BTS_012 was observed, confirming maximal abundance of this species in conjunction with undergoing process perturbations. In T07, with resumed reactor operation, an increase in cumulative abundance of beta-oxidation and WL pathway was observed. T07 was also characterized by a shift affecting the most abundant MAGs, as Limnochordia sp. BTS_001 and Bacillota_G sp. BTS_004 declined, while Dethiobacteria sp. BTS_008 peaked at RA 7.86 %. Class Dethiobacteria were previously proposed as SAOB [73], indeed MAG Dethiobacteria sp. BTS_008 had a complete WL pathway as well as a 1-bm WL/GCS, supporting this hypothesis. Its maximal abundance in T07 could thus represent the declining phase of an unobserved peak between T06 and T07. Such an increased abundance in Dethiobacteria sp. BTS_008 would lead to increased consumption of acetate, causing the low acetate levels observed in T07. Indeed, the MAG was found to be negatively correlated with acetate levels in the digestate (ρ_s −0.72, p-value 0.030, **Supplementary Figure S8**).

The GAL community displayed the highest abundance of cellulolytic *Herbivorax* and *Mobilitalea* bacteria owing to the pure silage feedstock. A noticeable drop in temperature of about 3 °C from the average occurred at T08. At that point, abundance reached the minimum for putative syntrophs Bacteria sp. BTS_010 and Dethiobacteria sp. BTS_008. Conversely, a sudden spike for fermentative Dysgonomonadaceae sp. BTS_002 happened and was maintained through to the next sampling point. *S. thermopropionivorans* BTS_012, previously absent from the reactor, appeared in the following points (T09, T10).

3.6.3. Chicken-manure digesting community at elevated FAN

PRO and GRE, characterized by the elevated FAN levels, displayed the lowest cumulative RA of MAGs with complete WL pathway for acetate oxidation. As the syntrophy between SAOB and hydrogenotrophs is the prevalent mechanism for methanogenesis in reactors with elevated FAN [43], a role for the alternative WL/GCS pathway is likely, which indeed was widely detected. GRE was characterized by the highest ratio between hydrolytic-fermentative bacteria and VFA oxidizers, explaining the elevated VFA levels. Indeed, acid content dropped at T07 when the abundance of oxidizers displayed a sudden peak. Metabolism of intermediates could be attributed to multiple Limnochordia MAGs via the WL/GCS pathway for SAOB and the custom module for butyrate oxidation. A similar activity could also be attributed to *Bacteroidales* sp. BTS_040 in addition to propionate oxidation. The most abundant MAG identified in reactor GRE, Fastidiosipilaceae sp. BTS_024 (order Saccharofermentanales) is a poorly characterized taxon. The type species

Fastidiosipila sanguinis was found to produce VFA without carbohydrate usage [68] and *Fastidiosipila* spp. were found with high RA in proteolytic AD communities [69–71]. Given the rich protein content of reactor GRE feedstock, we hypothesize this MAG to act as proteolytic. Indeed, two secreted peptidases were identified in its genome, alongside a moderate number of CAZymes (Fig. 3**A**). Similarly, the other Saccharofermentanales MAGs might act as proteolytic, as they were found to lack CAZymes and propionate or butyrate oxidation modules, while having a similar number of secreted peptidases. Erysipelotrichaceae were previously proposed to act as polysaccharide hydrolyzer, releasing VFA [72], although our analysis revealed a limited number of genes encoding for CAZymes (Fig. 3**A**).

Degradation of proteins in the reactors by means of secreted proteases is expected to be linked to AA degradation genes in the MAGs involved in this process and can determine an increase in ammonia (**Supplementary Figure S10**). Considering the vastly different levels of TAN across reactors, abundance of MAGs with complete modules for nitrogen metabolism was also calculated (**Supplementary Figure S11**). A high percentage of the community was found to encode for complete nitrogen metabolism modules in AGR, especially for "assimilatory nitrate reduction" and "dissimilatory nitrate reduction", as well as "nitrate assimilation". The latter was discovered to be largely absent from MAGs in GRE and PRO. Further, a functional enrichment analysis revealed the ammonium transporter gene *amt* to be overrepresented in the MAGs with average RA>1% exclusive to AGR, possibly explaining their presence in the nitrogen-poor environment (**Supplementary Figure S12**).

3.7. Archaeal diversity and dynamics

Archaeal presence was analyzed over time to evaluate their specificity and in order to understand their behavior according to changes in the feedstock composition (Fig. 5). The methanogenic component was very low in RA but varying between reactors, representing between 0.1 % (PRO) and 1 % (AGR) of the community (Fig. 3**C**). Eleven Archaeal MAGs were identified, and their activity classified according to taxonomy and functional annotation. Six *Methanoculleus* and two *Methanobacterium* MAGs were categorized as hydrogenotrophs, while Methanomassiliicoccaceae sp. BTS_110 as methylotroph. Finally, MAG *Methanosarcina flavescens* BTS_107, a known mixotroph, was the only archaeon capable of acetoclastic methanogenesis in addition to using H_2 and methyl compounds [73]. Finally, MAG Bathyarchaeia sp. BTS_114 was identified in reactor AGR and this taxon was previously regarded as

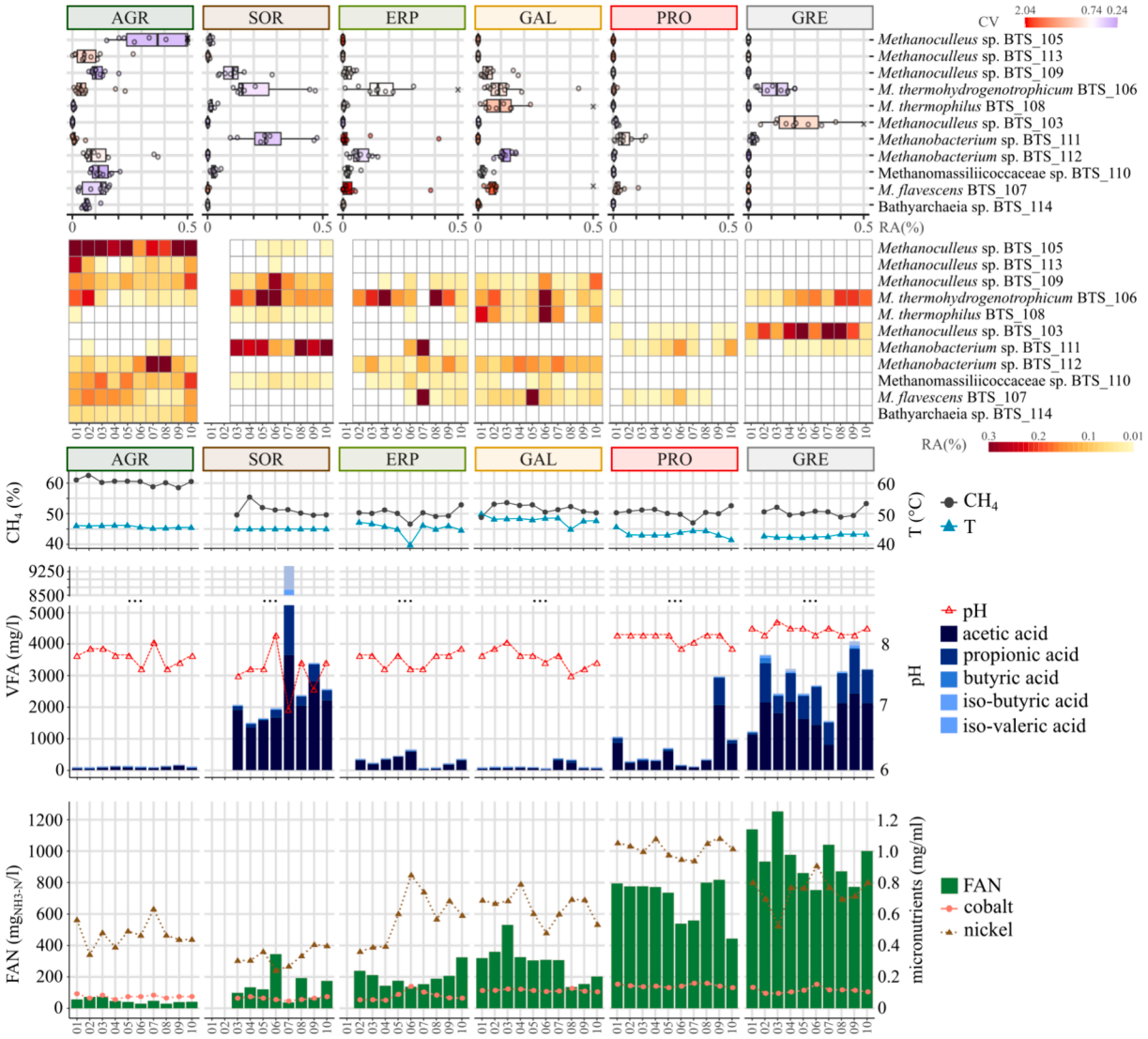

Fig. 5. Abundance of methanogenic archaea over time and with selected operating parameters. From the top: the first panel visualizes MAG's stability over time as a boxplot of RA and calculated Coefficient of Variation (CV) represented on a color scale. Second panel is a heatmap representing the RA of each MAG at different timepoints. The bottom three panels represent selected operational parameters at each time point.

a non-methanogenic methylotroph capable of growth on complex substrates including lignin [74].

The MAG assigned to *Candidatus* Methanoculleus thermohydrogenotrophicum (ANI 99.6 %) [75], *M. thermohydrogenotrophicum* BTS_106, was found in significant quantities (average RA>0.05 %) in all reactors suggesting a high resilience across different feedstocks and operating parameters. Plant PRO was an exception, which however had the lowest overall archaeal presence. Comparing the results with a previous large-scale characterization of the AD microbiome [21], this candidatus species was the second most widespread methanogen identified after an uncharacterized *Methanothrix* MAG. As the database did not include industrial olive–pomace digesting plants, this study further expands on the prevalence of *Candidatus* M. thermohydrogenotrophicum, including this peculiar substrate and underscoring the impressive adaptability of this interesting archaeon.

Cumulatively, the highest RA of methanogens in AGR mirrored the highest percentage of methane in the biogas. AGR displayed the largest heterogeneity in Archaea, as eight MAGs had average RA over 0.02 %. This finding resembled the general diversity measured for the microbiomes and contradicts the general idea that a selective environment, determined by high lipid and phenolic compounds concentration, can decrease the alpha diversity. Notably, two of these MAGs were not found in the Biogas Microbiome database and were also absent (average RA<0.02 %) from the other reactors. The first, *Methanoculleus* sp. BTS_105, was the dominant archaeon in AGR (average RA 0.37 %) and was classified as *Methanoculleus* sp002497965 (ANI 95.99 %), which was recently found partnering with a SPOB for propionate degradation in synthetic wastewater [76]. Notably, the dominant microbiome of reactor AGR displayed the highest RA of putative propionate degrading MAGs (Fig. 4), possibly explaining its exclusive presence and dominance in digesting olive pomace, in particular in association with *Candidatus* S. thermopropionivorans. Chicken manure-fed reactors GRE and PRO presented a less heterogeneous methanogenic community as compared to the other reactors. GRE was found to be exclusively reliant on hydrogenotrophic methanogenesis, mainly performed by the MAG *Methanoculleus* sp. BTS_103, which was also detected (>0.01 %) only in PRO, and the widespread *M. thermohydrogenotrophicum* BTS_106. *M. flavescens* BTS_107 was absent from reactor GRE possibly owing to the high FAN content inhibiting acetoclastic methanogens. These results showcase *Methanoculleus* genus as a flexible and fundamental taxon of the industrial AD process across diverse feedstocks and conditions at intermediate temperatures. In particular, *Candidatus* M. thermohydrogenotrophicum was capable of dominating in the most diverse conditions, while the specific presence of other *Methanoculleus* MAGs was determined by the feedstock or by other environmental conditions.

When considering variations across the monitored period, we noticed a seasonality trend in plant AGR, with a fluctuation in the methanogenic community possibly linked with the storage of olive pomace. In particular, hydrogenotrophs represented the largest proportion of all methanogens from August to November (maximum 0.88) while their predominance was lower from December to June (minimum 0.64) (**Supplementary Figure S5**). In plant ERP, following engine failure at T06, a severe drop in acetate levels in T07 co-occured with the shift in dominance from *M. thermohydrogenotrophicum* BTS_106 to a sporadic and intense appearance of *M. flavescens* BTS_107. It is possible that blooming of this acetoclastic archaeon was due to the accumulation of acetate and the lowering of temperature occurred at T06. With an increased abundance between T06 and T07, *M. flavescens* BTS_107 would consume the acetate leading to the low levels observed at T07. Such finding would confirm the effectiveness of *Methanosarcina* in relieving digesters from accumulated acetate [77]. It must be noted that *M. flavescens* BTS_107 exhibited a spike in abundance in reactors fed with a high percentage of silage (ERP, GAL, PRO) between April (T05) and August (T07). The temperature drop observed in GAL at point T08 lead to the minimum cumulative RA of archaea, but the constant presence of CH_4 in the biogas indicates that the community nevertheless adapted towards a sustained productivity.

4. Conclusions

This study compared the microbiome of six industrial AD plants with widely different feedstocks and operating parameters, including digesters operating on uncommon biomasses. The microbial communities were found to notably diverge in reactors fed with chicken manure and olive pomace operating with different levels of FAN/TAN and VFA, suggesting benefits for specialized inocula to efficiently operate on these organic wastes, while manure co-digestion appeared highly compatible with silage-digesting microbiomes. A set of MAGs was identified as putative core players of industrial AD, making them highly desirable in inocula destined for AD at 45 °C regardless of the digested input. Feedstock was found to affect microbiome stability, in particular a strong seasonality was found in the community digesting two-phase olive pomace, while operational parameters well explained differences across reactors. Alterations in the community were highlighted in conjunction with peculiar episodes related to changes in reactor operation and feedstock. Community simplification emerged as a potential factor favoring reactor acidification and relevant microbial markers of process instability were identified. The implementation of hybrid long and short-read shotgun sequencing unveiled distinct MAGs within the *Methanoculleus* genus showcasing either widespread or extremely niche presence. These findings underscore the versatility and pivotal role of the *Methanoculleus* genus as a key methanogen in AD processes across varied feedstocks and environmental conditions at 45 °C.

Overall, information on the relationship between reactor environment and microbiome will provide useful information for more rational management of full-scale biogas plants. Additionally, this study reinforces the idea that a monitoring process based not only on the physical and chemical parameters but also on the microbiological composition of the process is highly beneficial.

CRediT authorship contribution statement

D. Santinello: Writing – review & editing, Writing – original draft, Validation, Software, Investigation, Formal analysis. **G. Zampieri:** Writing – review & editing, Investigation, Data curation. **S. Agostini:** Investigation, Data curation. **B. Müller:** Resources, Funding acquisition. **L. Favaro:** Writing – review & editing, Funding acquisition, Conceptualization. **L. Treu:** Writing – review & editing, Supervision, Resources, Funding acquisition, Conceptualization. **S. Campanaro:** Writing – review & editing, Supervision, Resources, Funding acquisition, Conceptualization.

Declaration of competing interest

The authors declare that they have no known competing financial interests or personal relationships that could have appeared to influence the work reported in this paper.

Data availability

Raw data from metagenomic analyses generated in this study have been deposited in the NCBI under BioProject number PRJNA1101514.

Acknowledgments

This work was supported by Fondazione Cariverona under the Call for Research project “Più-BIOGAS App: sviluppo di strategie innovative per ottimizzare la produzione di energia rinnovabile da scarti agro-alimentari”, grant C25F20000520003, and by the project “L’innovazione delle Biotecnologie nell’Era della Medicina di Precisione, dei Cambiamenti climatici e dell’Economia Circolare” (MUR ex D.M. 1059 d.d 09/08/2021) of the Consorzio Interuniversitario per le

Biotecnologie (CIB). We acknowledge Italiana Biotecnologie s.r.l. for the support.

Appendix A. Supplementary data

Supplementary data to this article can be found online at https://doi.org/10.1016/j.cej.2024.154962.

References

[1] J.M. Clomburg, A.M. Crumbley, R. Gonzalez, Industrial biomanufacturing: The future of chemical production, Science 355 (2017) aag0804, https://doi.org/10.1126/science.aag0804.

[2] J. Song, Y. Wang, S. Zhang, Y. Song, S. Xue, L. Liu, X. Lvy, X. Wang, G. Yang, Coupling biochar with anaerobic digestion in a circular economy perspective: A promising way to promote sustainable energy, environment and agriculture development in China, Renew. Sustain. Energy Rev. 144 (2021) 110973, https://doi.org/10.1016/j.rser.2021.110973.

[3] M. Rasapoor, B. Young, R. Brar, A. Sarmah, W.-Q. Zhuang, S. Baroutian, Recognizing the challenges of anaerobic digestion: Critical steps toward improving biogas generation, Fuel 261 (2020) 116497, https://doi.org/10.1016/j.fuel.2019.116497.

[4] M.R. Atelge, D. Krisa, G. Kumar, C. Eskicioglu, D.D. Nguyen, S.W. Chang, A. E. Atabani, A.H. Al-Muhtaseb, S. Unalan, Biogas Production from Organic Waste: Recent Progress and Perspectives, Waste Biomass Valorization 11 (2020) 1019–1040, https://doi.org/10.1007/s12649-018-00546-0.

[5] F. Mayer, V. Müller, Adaptations of anaerobic archaea to life under extreme energy limitation, FEMS Microbiol. Rev. 38 (2014) 449–472, https://doi.org/10.1111/1574-6976.12043.

[6] L. Lin, F. Xu, X. Ge, Y. Li, Improving the sustainability of organic waste management practices in the food-energy-water nexus: A comparative review of anaerobic digestion and composting, Renew. Sustain. Energy Rev. 89 (2018) 151–167, https://doi.org/10.1016/j.rser.2018.03.025.

[7] J. Vasco-Correa, S. Khanal, A. Manandhar, A. Shah, Anaerobic digestion for bioenergy production: Global status, environmental and techno-economic implications, and government policies, Bioresour. Technol. 247 (2018) 1015–1026, https://doi.org/10.1016/j.biortech.2017.09.004.

[8] S. Agostini, L. Bucci, D. Doni, P. Costantini, A. Gupte, B. Müller, F. Sibilla, M. Basaglia, S. Casella, P.G. Kougias, S. Campanaro, L. Favaro, L. Treu, Bioaugmentation strategies based on bacterial and methanogenic cultures to relieve stress in anaerobic digestion of protein-rich substrates, (2023) 2023.12.11.571062. doi: 10.1101/2023.12.11.571062.

[9] A.J. Ward, P.J. Hobbs, P.J. Holliman, D.L. Jones, Optimisation of the anaerobic digestion of agricultural resources, Bioresour. Technol. 99 (2008) 7928–7940, https://doi.org/10.1016/j.biortech.2008.02.044.

[10] D. De Francisci, P.G. Kougias, L. Treu, S. Campanaro, I. Angelidaki, Microbial diversity and dynamicity of biogas reactors due to radical changes of feedstock composition, Bioresour. Technol. 176 (2015) 56–64, https://doi.org/10.1016/j.biortech.2014.10.126.

[11] M. Madsen, J.B. Holm-Nielsen, K.H. Esbensen, Monitoring of anaerobic digestion processes: A review perspective, Renew. Sustain. Energy Rev. 15 (2011) 3141–3155, https://doi.org/10.1016/j.rser.2011.04.026.

[12] S.T. Oh, A.D. Martin, Thermodynamic equilibrium model in anaerobic digestion process, Biochem. Eng. J. 34 (2007) 256–266, https://doi.org/10.1016/j.bej.2006.12.011.

[13] D. Rivière, V. Desvignes, E. Pelletier, S. Chaussonnerie, S. Guermazi, J. Weissenbach, T. Li, P. Camacho, A. Sghir, Towards the definition of a core of microorganisms involved in anaerobic digestion of sludge, ISME J. 3 (2009) 700–714, https://doi.org/10.1038/ismej.2009.2.

[14] C. Yang, D. Chowdhury, Z. Zhang, W.K. Cheung, A. Lu, Z. Bian, L. Zhang, A review of computational tools for generating metagenome-assembled genomes from metagenomic sequencing data, Comput. Struct, Biotechnol. J. 19 (2021) 6301–6314, https://doi.org/10.1016/j.csbj.2021.11.028.

[15] S. Campanaro, L. Treu, L.M. Rodriguez-R, A. Kovalovszki, R.M. Ziels, I. Maus, X. Zhu, P.G. Kougias, A. Basile, G. Luo, A. Schlüter, K.T. Konstantinidis, I. Angelidaki, New insights from the biogas microbiome by comprehensive genome-resolved metagenomics of nearly 1600 species originating from multiple anaerobic digesters, Biotechnol. Biofuels 13 (2020) 25, https://doi.org/10.1186/s13068-020-01679-y.

[16] I.W. Koster, Characteristics of the pH-influenced adaptation of methanogenic sludge to ammonium toxicity, J. Chem. Technol. Biotechnol. 36 (1986) 445–455, https://doi.org/10.1002/jctb.280361003.

[17] G. Zampieri, S. Campanaro, C. Angione, L. Treu, Metatranscriptomics-guided genome-scale metabolic modeling of microbial communities, Cell Rep. Methods 3 (2023) 100383, https://doi.org/10.1016/j.crmeth.2022.100383.

[18] R.M. Bowers, N.C. Kyrpides, R. Stepanauskas, M. Harmon-Smith, D. Doud, T.B. K. Reddy, F. Schulz, J. Jarett, A.R. Rivers, E.A. Eloe-Fadrosh, S.G. Tringe, N. N. Ivanova, A. Copeland, A. Clum, E.D. Becraft, R.R. Malmstrom, B. Birren, M. Podar, P. Bork, G.M. Weinstock, G.M. Garrity, J.A. Dodsworth, S. Yooseph, G. Sutton, F.O. Glöckner, J.A. Gilbert, W.C. Nelson, S.J. Hallam, S.P. Jungbluth, T. J.G. Ettema, S. Tighe, K.T. Konstantinidis, W.-T. Liu, B.J. Baker, T. Rattei, J. A. Eisen, B. Hedlund, K.D. McMahon, N. Fierer, R. Knight, R. Finn, G. Cochrane, I. Karsch-Mizrachi, G.W. Tyson, C. Rinke, A. Lapidus, F. Meyer, P. Yilmaz, D. H. Parks, A. Murat Eren, L. Schriml, J.F. Banfield, P. Hugenholtz, T. Woyke, Minimum information about a single amplified genome (MISAG) and a metagenome-assembled genome (MIMAG) of bacteria and archaea, Nat. Biotechnol. 35 (2017) 725–731, https://doi.org/10.1038/nbt.3893.

[19] P.J. McMurdie, S. Holmes, phyloseq: An R Package for Reproducible Interactive Analysis and Graphics of Microbiome Census Data, PLOS ONE 8 (2013) e61217.

[20] P.-A. Chaumeil, A.J. Mussig, P. Hugenholtz, D.H. Parks, GTDB-Tk: a toolkit to classify genomes with the Genome Taxonomy Database, Bioinformatics 36 (2020) 1925–1927, https://doi.org/10.1093/bioinformatics/btz848.

[21] V.B. Centurion, A. Rossi, E. Orellana, G. Ghiotto, B. Kakuk, M.S. Morlino, A. Basile, G. Zampieri, L. Treu, S. Campanaro, A unified compendium of prokaryotic and viral genomes from over 300 anaerobic digestion microbiomes, Environ. Microbiome 19 (2024) 1, https://doi.org/10.1186/s40793-023-00545-2.

[22] M.R. Olm, C.T. Brown, B. Brooks, J.F. Banfield, dRep: a tool for fast and accurate genomic comparisons that enables improved genome recovery from metagenomes through de-replication, ISME J. 11 (2017) 2864–2868, https://doi.org/10.1038/ismej.2017.126.

[23] A. Chklovski, D.H. Parks, B.J. Woodcroft, G.W. Tyson, CheckM2: a rapid, scalable and accurate tool for assessing microbial genome quality using machine learning, Nat. Methods 20 (2023) 1203–1212, https://doi.org/10.1038/s41592-023-01940-w.

[24] D. Hyatt, G.-L. Chen, P.F. LoCascio, M.L. Land, F.W. Larimer, L.J. Hauser, Prodigal: prokaryotic gene recognition and translation initiation site identification, BMC Bioinformatics 11 (2010) 119, https://doi.org/10.1186/1471-2105-11-119.

[25] C.P. Cantalapiedra, A. Hernández-Plaza, I. Letunic, P. Bork, J. Huerta-Cepas, eggNOG-mapper v2: Functional Annotation, Orthology Assignments, and Domain Prediction at the Metagenomic Scale, Mol. Biol. Evol. 38 (2021) 5825–5829, https://doi.org/10.1093/molbev/msab293.

[26] J. Zheng, Q. Ge, Y. Yan, X. Zhang, L. Huang, Y. Yin, dbCAN3: automated carbohydrate-active enzyme and substrate annotation, Nucleic Acids Res. 51 (2023) W115–W121, https://doi.org/10.1093/nar/gkad328.

[27] M. Kanehisa, S. Goto, KEGG: Kyoto Encyclopedia of Genes and Genomes, Nucleic Acids Res. 28 (2000) 27–30, https://doi.org/10.1093/nar/28.1.27.

[28] F. Asnicar, A.M. Thomas, F. Beghini, C. Mengoni, S. Manara, P. Manghi, Q. Zhu, M. Bolzan, F. Cumbo, U. May, J.G. Sanders, M. Zolfo, E. Kopylova, E. Pasolli, R. Knight, S. Mirarab, C. Huttenhower, N. Segata, Precise phylogenetic analysis of microbial isolates and genomes from metagenomes using PhyloPhlAn 3.0, Nat. Commun. 11 (2020) 2500, https://doi.org/10.1038/s41467-020-16366-7.

[29] I. Letunic, P. Bork, Interactive Tree Of Life (iTOL) v5: an online tool for phylogenetic tree display and annotation, Nucleic Acids Res. 49 (2021) W293–W296, https://doi.org/10.1093/nar/gkab301.

[30] N.Y. Yu, J.R. Wagner, M.R. Laird, G. Melli, S. Rey, R. Lo, P. Dao, S.C. Sahinalp, M. Ester, L.J. Foster, F.S.L. Brinkman, PSORTb 3.0: improved protein subcellular localization prediction with refined localization subcategories and predictive capabilities for all prokaryotes, Bioinformatics 26 (2010) 1608–1615, https://doi.org/10.1093/bioinformatics/btq249.

[31] A. Weimann, K. Mooren, J. Frank, P.B. Pope, A. Bremges, A.C. McHardy, From Genomes to Phenotypes: Traitar, the Microbial Trait Analyzer, mSystems 1 (2016) 10.1128/msystems.00101-16. doi: 10.1128/msystems.00101-16.

[32] J. Oksanen, G.L. Simpson, F.G. Blanchet, R. Kindt, P. Legendre, P.R. Minchin, R. B. O'Hara, P. Solymos, M.H.H. Stevens, E. Szoecs, H. Wagner, M. Barbour, M. Bedward, B. Bolker, D. Borcard, G. Carvalho, M. Chirico, M.D. Caceres, S. Durand, H.B.A. Evangelista, R. FitzJohn, M. Friendly, B. Furneaux, G. Hannigan, M.O. Hill, L. Lahti, D. McGlinn, M.-H. Ouellette, E.R. Cunha, T. Smith, A. Stier, C.J. F.T. Braak, accessed March 19, 2024, J. Weedon, Vegan: Community Ecology Package (2022), https://cran.r-project.org/web/packages/vegan/.

[33] J.R. Conway, A. Lex, N. Gehlenborg, UpSetR: an R package for the visualization of intersecting sets and their properties, Bioinformatics 33 (2017) 2938–2940, https://doi.org/10.1093/bioinformatics/btx364.

[34] J. Boyd, geronimp/enrichM, (2024). https://github.com/geronimp/enrichM (accessed March 6, 2024).

[35] S. Hupfauf, A. Winkler, A.O. Wagner, S.M. Podmirseg, H. Insam, Biomethanation at 45 °C offers high process efficiency and supports hygienisation, Bioresour. Technol. 300 (2020) 122671, https://doi.org/10.1016/j.biortech.2019.122671.

[36] A.M. Ziganshin, J. Liebetrau, J. Pröter, S. Kleinsteuber, Microbial community structure and dynamics during anaerobic digestion of various agricultural waste materials, Appl. Microbiol. Biotechnol. 97 (2013) 5161–5174, https://doi.org/10.1007/s00253-013-4867-0.

[37] F. Abouelenien, W. Fujiwara, Y. Namba, M. Kosseva, N. Nishio, Y. Nakashimada, Improved methane fermentation of chicken manure via ammonia removal by biogas recycle, Bioresour. Technol. 101 (2010) 6368–6373, https://doi.org/10.1016/j.biortech.2010.03.071.

[38] D. Thanos, A. Maragkaki, D. Venieri, M. Fountoulakis, T. Manios, Enhanced Biogas Production in Pilot Digesters Treating a Mixture of Olive Mill Wastewater and Agro-industrial or Agro-livestock By-Products in Greece, Waste Biomass Valorization 12 (2021) 135–143, https://doi.org/10.1007/s12649-020-00963-0.

[39] D. Traversi, V. Romanazzi, R. Degan, E. Lorenzi, E. Carraro, G. Gilli, Microbial-chemical indicator for anaerobic digester performance assessment in full-scale wastewater treatment plants for biogas production, Bioresour. Technol. 186 (2015) 179–191, https://doi.org/10.1016/j.biortech.2015.03.042.

[40] R. Nkuna, A. Roopnarain, C. Rashama, R. Adeleke, Insights into organic loading rates of anaerobic digestion for biogas production: a review, Crit. Rev. Biotechnol. 42 (2022) 487–507, https://doi.org/10.1080/07388551.2021.1942778.

[41] I. Angelidaki, B.K. Ahring, Anaerobic thermophilic digestion of manure at different ammonia loads: Effect of temperature, Water Res. 28 (1994) 727–731, https://doi.org/10.1016/0043-1354(94)90153-8.

[42] D.-M. Yin, M. Westerholm, W. Qiao, S.-J. Bi, S.M. Wandera, R. Fan, M.-M. Jiang, R.-J. Dong, An explanation of the methanogenic pathway for methane production in anaerobic digestion of nitrogen-rich materials under mesophilic and thermophilic conditions, Bioresour. Technol. 264 (2018) 42–50, https://doi.org/10.1016/j.biortech.2018.05.062.
[43] M. Westerholm, J. Moestedt, A. Schnürer, Biogas production through syntrophic acetate oxidation and deliberate operating strategies for improved digester performance, Appl. Energy 179 (2016) 124–135, https://doi.org/10.1016/j.apenergy.2016.06.061.
[44] J. De Vrieze, A.M. Saunders, Y. He, J. Fang, P.H. Nielsen, W. Verstraete, N. Boon, Ammonia and temperature determine potential clustering in the anaerobic digestion microbiome, Water Res. 75 (2015) 312–323, https://doi.org/10.1016/j.watres.2015.02.025.
[45] G. Ghiotto, G. Zampieri, S. Campanaro, L. Treu, Strain-resolved metagenomics approaches applied to biogas upgrading, Environ. Res. 240 (2024) 117414, https://doi.org/10.1016/j.envres.2023.117414.
[46] R. Serna-García, P. Tsapekos, L. Treu, A. Bouzas, A. Seco, S. Campanaro, I. Angelidaki, Unraveling prevalence of homoacetogenesis and methanogenesis pathways due to inhibitors addition, Bioresour. Technol. 376 (2023) 128922, https://doi.org/10.1016/j.biortech.2023.128922.
[47] E.A. Zhuravleva, S.V. Shekhurdina, I.B. Kotova, N.G. Loiko, N.M. Popova, E. Kryukov, A.A. Kovalev, D.A. Kovalev, Y.V. Litti, Effects of various materials used to promote the direct interspecies electron transfer on anaerobic digestion of low-concentration swine manure, Sci. Total Environ. 839 (2022) 156073, https://doi.org/10.1016/j.scitotenv.2022.156073.
[48] L. Treu, S. Campanaro, P.G. Kougias, C. Sartori, I. Bassani, I. Angelidaki, Hydrogen-Fueled Microbial Pathways in Biogas Upgrading Systems Revealed by Genome-Centric Metagenomics, accessed February 27, 2023, Front. Microbiol. 9 (2018), https://www.frontiersin.org/articles/10.3389/fmicb.2018.01079.
[49] F. Mosbæk, H. Kjeldal, D.G. Mulat, M. Albertsen, A.J. Ward, A. Feilberg, J. L. Nielsen, Identification of syntrophic acetate-oxidizing bacteria in anaerobic digesters by combined protein-based stable isotope probing and metagenomics, ISME J. 10 (2016) 2405–2418, https://doi.org/10.1038/ismej.2016.39.
[50] N. De Bernardini, A. Basile, G. Zampieri, A. Kovalovszki, B. De Diego Diaz, E. Offer, N. Wongfaed, I. Angelidaki, P.G. Kougias, S. Campanaro, L. Treu, Integrating metagenomic binning with flux balance analysis to unravel syntrophies in anaerobic CO2 methanation, Microbiome 10 (2022) 117, https://doi.org/10.1186/s40168-022-01311-1.
[51] S. Agostini, F. Moriconi, M. Zampirolli, D. Padoan, L. Treu, S. Campanaro, L. Favaro, Monitoring the Microbiomes of Agricultural and Food Waste Treating Biogas Plants over a One-Year Period, Appl. Sci. 13 (2023) 9959, https://doi.org/10.3390/app13179959.
[52] I. Owusu-Agyeman, E. Plaza, Z. Cetecioglu, Long-term alkaline volatile fatty acids production from waste streams: Impact of pH and dominance of *Dysgonomonadaceae*, Bioresour. Technol. 346 (2022) 126621, https://doi.org/10.1016/j.biortech.2021.126621.
[53] S. Dyksma, C. Gallert, Candidatus Syntrophosphaera thermopropionivorans: a novel player in syntrophic propionate oxidation during anaerobic digestion, Environ. Microbiol. Rep. 11 (2019) 558–570, https://doi.org/10.1111/1758-2229.12759.
[54] Y.V. Litti, D.A. Kovalev, A.A. Kovalev, A.Y. Merkel, A.V. Vishnyakova, Y. I. Russkova, A.N. Nozhevnikova, Auto-selection of microorganisms of sewage sludge used as an inoculum for fermentative hydrogen production from different substrates, Int. J. Hydrog. Energy 46 (2021) 29834–29845, https://doi.org/10.1016/j.ijhydene.2021.06.174.
[55] T. Yamada, Y. Sekiguchi, S. Hanada, H. Imachi, A. Ohashi, H. Harada, Y. Kamagata, Anaerolinea thermolimosa sp. nov., Levilinea saccharolytica gen. nov., sp. nov. and Leptolinea tardivitalis gen. nov., sp. nov., novel filamentous anaerobes, and description of the new classes Anaerolineae classis nov. and Caldilineae classis nov. in the bacterial phylum Chloroflexi, Int. J. Syst. Evol. Microbiol. 56 (2006) 1331–1340. doi: 10.1099/ijs.0.64169-0.
[56] B. Liang, L.-Y. Wang, S.M. Mbadinga, J.-F. Liu, S.-Z. Yang, J.-D. Gu, B.-Z. Mu, Anaerolineaceae and Methanosaeta turned to be the dominant microorganisms in alkanes-dependent methanogenic culture after long-term of incubation, AMB Express 5 (2015) 37, https://doi.org/10.1186/s13568-015-0117-4.
[57] F. Petriglieri, M. Nierychlo, P.H. Nielsen, S.J. McIlroy, In situ visualisation of the abundant Chloroflexi populations in full-scale anaerobic digesters and the fate of immigrating species, PLOS ONE 13 (2018) e0206255.
[58] S.J. McIlroy, R.H. Kirkegaard, M.S. Dueholm, E. Fernando, S.M. Karst, M. Albertsen, P.H. Nielsen, Culture-Independent Analyses Reveal Novel Anaerolineaceae as Abundant Primary Fermenters in Anaerobic Digesters Treating Waste Activated Sludge, accessed March 1, 2024, Front. Microbiol. 8 (2017), https://www.frontiersin.org/journals/microbiology/articles/10.3389/fmicb.2017.01134.
[59] S. Kagemasa, K. Kuroda, R. Nakai, Y.-Y. Li, K. Kubota, Diversity of *Candidatus* Patescibacteria in Activated Sludge Revealed by a Size-Fractionation Approach, Microbes Environ. 37 (2022) ME22027, https://doi.org/10.1264/jsme2.ME22027.
[60] C.J. Castelle, C.T. Brown, K. Anantharaman, A.J. Probst, R.H. Huang, J.F. Banfield, Biosynthetic capacity, metabolic variety and unusual biology in the CPR and DPANN radiations, Nat. Rev. Microbiol. 16 (2018) 629–645, https://doi.org/10.1038/s41579-018-0076-2.
[61] K. Kuroda, S. Tomita, H. Kurashita, M. Hatamoto, T. Yamaguchi, T. Hori, T. Aoyagi, Y. Sato, T. Inaba, H. Habe, H. Tamaki, Y. Hagihara, T. Tamura, T. Narihiro, Metabolic implications for predatory and parasitic bacterial lineages in activated sludge wastewater treatment systems, Water Res. X 20 (2023) 100196, https://doi.org/10.1016/j.wroa.2023.100196.
[62] M. Calusinska, X. Goux, M. Fossépré, E.E.L. Muller, P. Wilmes, P. Delfosse, A year of monitoring 20 mesophilic full-scale bioreactors reveals the existence of stable but different core microbiomes in bio-waste and wastewater anaerobic digestion systems, Biotechnol. Biofuels 11 (2018) 196, https://doi.org/10.1186/s13068-018-1195-8.
[63] I. Rychlik, Composition and Function of Chicken Gut Microbiota, Anim. Open Access J. MDPI 10 (2020) 103, https://doi.org/10.3390/ani10010103.
[64] R. Sakurai, Y. Yokoyama, Y. Fukuda, C. Tada, Quantification of free and esterified long-chain fatty acids without extraction by high-performance liquid chromatography in anaerobic digestion sludge, J. Mater. Cycles Waste Manag. 25 (2023) 810–815, https://doi.org/10.1007/s10163-022-01561-z.
[65] D. Elalami, H. Carrere, K. Abdelouahdi, D. Garcia-Bernet, J. Peydecastaing, G. Vaca-Medina, A. Oukarroum, Y. Zeroual, A. Barakat, Mild microwaves, ultrasonic and alkaline pretreatments for improving methane production: Impact on biochemical and structural properties of olive pomace, Bioresour. Technol. 299 (2020) 122591, https://doi.org/10.1016/j.biortech.2019.122591.
[66] H. Zhao, D. Yang, C.R. Woese, M.P. Bryant, Assignment of Fatty Acid-ß-Oxidizing Syntrophic Bacteria to Syntrophomonadaceae fam. nov. on the Basis of 16S rRNA Sequence Analyses, Int. J. Syst. Evol. Microbiol. 43 (1993) 278–286, https://doi.org/10.1099/00207713-43-2-278.
[67] A. Christofi, P. Fella, A. Agapiou, E.M. Barampouti, S. Mai, K. Moustakas, M. Loizidou, The Impact of Drying and Storage on the Characteristics of Two-Phase Olive Pomace, Sustainability 16 (2024) 1116, https://doi.org/10.3390/su16031116.
[68] E. Falsen, M.D. Collins, C. Welinder-Olsson, Y. Song, S.M. Finegold, P.A. Lawson, Fastidiosipila sanguinis gen. nov., sp. nov., a new Gram-positive, coccus-shaped organism from human blood, Int. J. Syst. Evol. Microbiol. 55 (2005) 853–858, https://doi.org/10.1099/ijs.0.63327-0.
[69] S. Chen, B. Dong, X. Dai, H. Wang, N. Li, D. Yang, Effects of thermal hydrolysis on the metabolism of amino acids in sewage sludge in anaerobic digestion, Waste Manag. 88 (2019) 309–318, https://doi.org/10.1016/j.wasman.2019.03.060.
[70] J. Cardinali-Rezende, P. Rojas-Ojeda, A.M.A. Nascimento, J.L. Sanz, Proteolytic bacterial dominance in a full-scale municipal solid waste anaerobic reactor assessed by 454 pyrosequencing technology, Chemosphere 146 (2016) 519–525, https://doi.org/10.1016/j.chemosphere.2015.12.003.
[71] E. Perman, A. Schnürer, A. Björn, J. Moestedt, Serial anaerobic digestion improves protein degradation and biogas production from mixed food waste, Biomass Bioenergy 161 (2022) 106478, https://doi.org/10.1016/j.biombioe.2022.106478.
[72] J. Wu, M. Liu, M. Zhou, L. Wu, H. Yang, L. Huang, C. Chen, Isolation and genomic characterization of five novel strains of Erysipelotrichaceae from commercial pigs, BMC Microbiol. 21 (2021) 125, https://doi.org/10.1186/s12866-021-02193-3.
[73] T. Kern, M.A. Fischer, U. Deppenmeier, R.A. Schmitz, M. Rother, Methanosarcina flavescens sp. nov., a methanogenic archaeon isolated from a full-scale anaerobic digester, Int. J. Syst. Evol. Microbiol. 66 (2016) 1533–1538, https://doi.org/10.1099/ijsem.0.000894.
[74] J. Hou, Y. Wang, P. Zhu, N. Yang, L. Liang, T. Yu, M. Niu, K. Konhauser, B. J. Woodcroft, F. Wang, Taxonomic and carbon metabolic diversification of Bathyarchaeia during its coevolution history with early Earth surface environment, Sci. Adv. 9 (2023) eadf5069, https://doi.org/10.1126/sciadv.adf5069.
[75] P.G. Kougias, S. Campanaro, L. Treu, X. Zhu, I. Angelidaki, A novel archaeal species belonging to *Methanoculleus* genus identified via de-novo assembly and metagenomic binning process in biogas reactors, Anaerobe 46 (2017) 23–32, https://doi.org/10.1016/j.anaerobe.2017.02.009.
[76] M. Kim, C. Rhee, M. Wells, J. Shin, J. Lee, S.G. Shin, Key players in syntrophic propionate oxidation revealed by metagenome-assembled genomes from anaerobic digesters bioaugmented with propionic acid enriched microbial consortia, Front. Microbiol. 13 (2022) 968416, https://doi.org/10.3389/fmicb.2022.968416.
[77] P. Lins, C. Reitschuler, P. Illmer, *Methanosarcina* spp., the key to relieve the start-up of a thermophilic anaerobic digestion suffering from high acetic acid loads, Bioresour. Technol. 152 (2014) 347–354, https://doi.org/10.1016/j.biortech.2013.11.020.